

*Supplementary Information***Reduction of Uncorrelated Striping Noise—Applications for Hyperspectral Pushbroom Acquisitions. *Remote Sensing*, 2014, 6, 11082–11106**

Christian Rogass ^{1,*}, Christian Mielke ¹, Daniel Scheffler ¹, Nina K. Boesche ¹, Angela Lausch ², Christin Lubitz ¹, Maximilian Brell ¹, Daniel Spengler ¹, Andreas Eisele ¹, Karl Segl ¹ and Luis Guanter ¹

- ¹. Helmholtz Center Potsdam, German Research Center for Geosciences, Telegrafenberg, Potsdam 14473, Germany; E-Mails: christian.mielke@gfz-potsdam.de (C.M.); daniel.scheffler@gfz-potsdam.de (D.S); nina.boesche@gfz-potsdam.de (N.B.); christin.lubitz@gfz-potsdam.de (C.L.); maximilian.brell@gfz-potsdam.de (M.B.); daniel.spengler@gfz-potsdam.de (D.S.); andreas.eisele@gfz-potsdam.de (A.E.); karl.segl@gfz-potsdam.de (K.S.); luis.guanter@gfz-potsdam.de (L.G.)
- ². Helmholtz Center for Environmental Research-UFZ, Permoserstr 15, Leipzig 04318, Germany; E-Mail: angela.lausch@ufz.de

* Author to whom correspondence should be addressed; E-Mail: christian.rogass@gfz-potsdam.de; Tel.: +49-331-288-1820; Fax: +49-331-288-1192.

Received: 5 September 2014; in revised form: 30 October 2014 / Accepted: 4 November 2014 /

Published: 11 November 2014

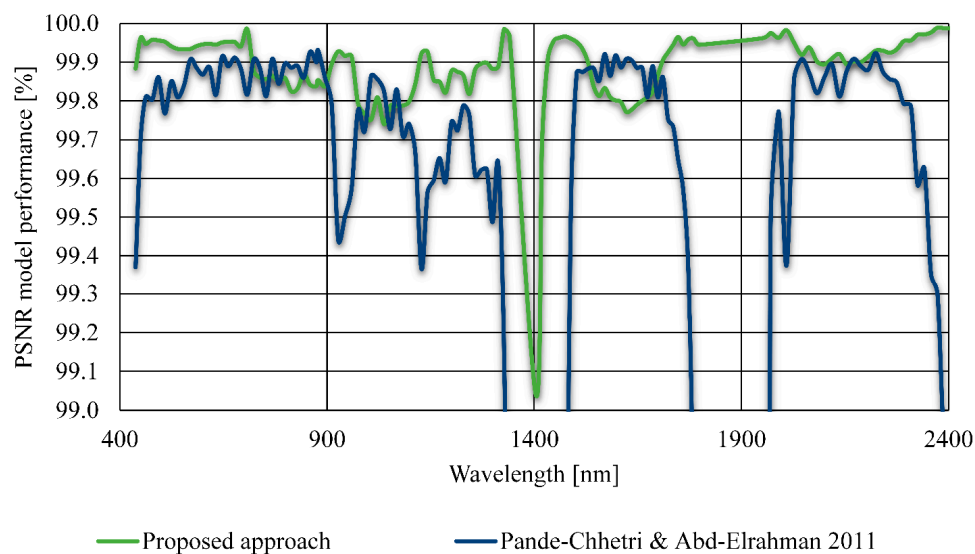
Supplementary Material

Additional figures are presented here to help the readers of the article to get a better understanding of the proposed methodology, comparisons and achieved results that has to be excluded from the main article to preserve the integrity and the compactness of the article.

Supplement 1

The PSNR was selected as one out of four indicators for the evaluation of the performance of tested approaches. Here, the results for the PSNR evaluation of two best approaches are shown.

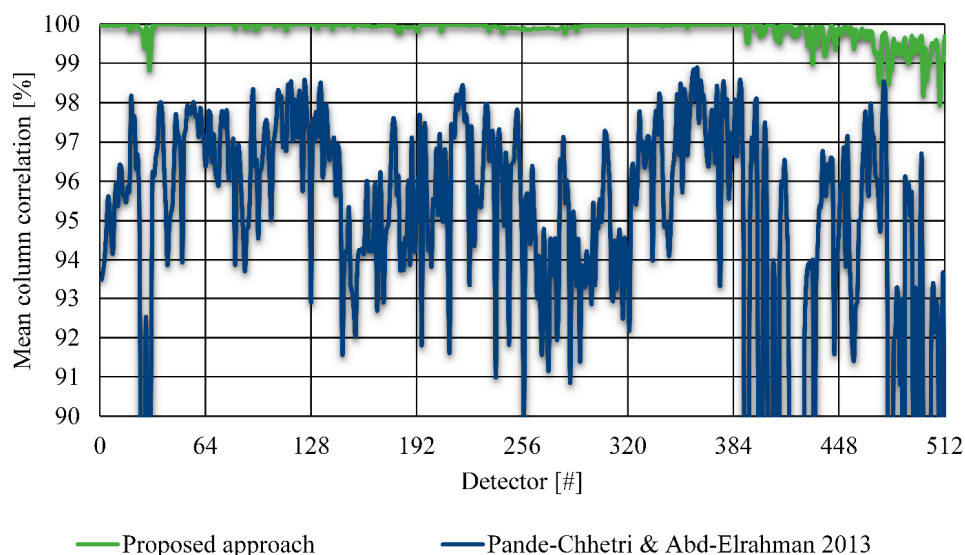
Figure S1. Average PSNR of the two best performing approaches for artificially degraded images [1].



Supplement 2

In addition to the PSNR the column correlation between adjacent columns has been selected for inclusion as performance indicator to consider slightly varying information of adjacent image columns.

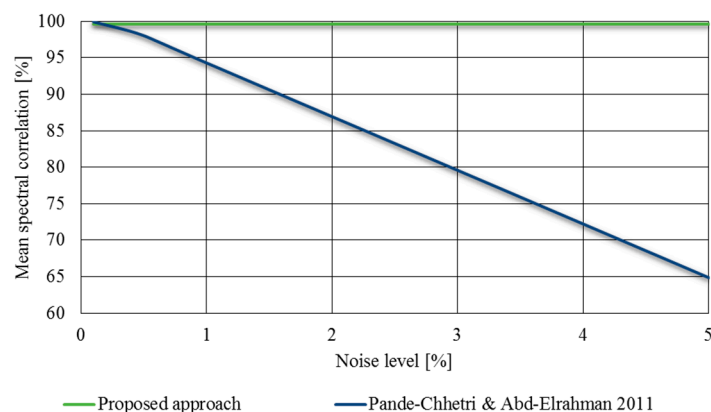
Figure S2. Column correlation of the two best performing approaches for artificially degraded images [2].



Supplement 3

In addition to the PSNR, the MSSIM and the mean column correlation the overall image correlation has been evaluated to provide a direct spectral metric between ground truth and the destriping results.

Figure S3. Overall correlation of the two best performing approaches for artificially degraded images [3].



Supplement 4

The following Supplementary Tables 4–6 give a tabulated overview for all achieved results. The results has been ranked according their indicator to give the readers of the article a better overview.

Table S4. Overall performance ranking for simulated images based on HyMAP data takes [4].

Approach/Indicator	M1	M2	M3	M4	M5	M6
PSNR [#]	1	4	3	6	2	5
SSIM [#]	1	4	3	5	2	6
Column Correlation [#]	1	4	5	6	3	2
Overall Correlation [#]	1	4	5	6	3	2
Visual comparison [#]	1	3	2	6	4	5
Average [#] (Σ)	1 (5)	4 (19)	3 (18)	6 (29)	2 (14)	5 (20)

M1: Proposed approach; M2: Rogass *et al.* (2012) [1]; M3: Goodenough *et al.* (2003) and Datt *et al.* (2003) [2,3]; M4: Staenz *et al.* (2002) [4]; M5: Pande-Chhetri and Abd-Elrahman (2011) [5]; M6: Pande-Chhetri and Abd-Elrahman (2013) [6].

Supplement 5

Table S5. Overall performance ranking for real Hyperion images [5].

Approach/Indicator	M1	M2	M3	M4	M5	M6
Median AAHPD/Hyperion [#]	1	2	3	5	4	6
Median CIAG/Hyperion [#]	1	2	4	3	5	6
Visual comparison Hyperion [#]	1	3	1	5	2	4
Average [#](Σ)	1 (3)	2 (6)	3 (8)	5 (13)	4 (11)	5 (16)

M1: Proposed approach; M2: Rogass *et al.* (2012) [1]; M3: Goodenough *et al.* (2003) and Datt *et al.* (2003) [2,3]; M4: Staenz *et al.* (2002) [4]; M5: Pande-Chhetri and Abd-Elrahman (2011) [5]; M6: Pande-Chhetri and Abd-Elrahman (2013) [6].

Supplement 6

Table S6. Overall performance ranking for real AISA images [6].

Approach/Indicator	M1	M2	M3	M4	M5	M6
Median AAHPD/AISA [#]	1	4	6	2	3	5
Median CIAG/AISA [#]	3	2	6	4	1	5
Visual comparison AISA [#]	1	5	1	3	4	2
Average [#](Σ)	<u>1 (5)</u>	<u>4 (11)</u>	<u>6 (13)</u>	<u>3 (9)</u>	<u>2 (8)</u>	<u>5 (12)</u>

M1: Proposed approach; M2: Rogass *et al.* (2012) [1]; M3: Goodenough *et al.* (2003) and Datt *et al.* (2003) [2,3]; M4: Staenz *et al.* (2002) [4]; M5: Pande-Chhetri and Abd-Elrahman (2011) [5]; M6: Pande-Chhetri and Abd-Elrahman (2013) [6]

References

1. Rogass, C.; Spengler, D.; Bochow, M.; Segl, K.; Lausch, A.; Doktor, D.; Roessner, S.; Behling, R.; Wetzel, H. U.; Urata, K.; Hueni, A.; Kaufmann, H. A Contribution to the Reduction of Radiometric Miscalibration of Pushbroom Sensors. Available online: http://www.researchgate.net/publication/229057638_Estimation_of_the_Separable_MGMRF_Parameters_for_Thematic_Classification#page=163 (accessed on 5 September 2014).
2. Goodenough, D. G.; Dyk, A.; Niemann, K.O.; Pearlman, J.S.; Chen, H.; Han, T.; Murdoch, M.; West, C. Processing Hyperion and ALI for forest classification. *IEEE Trans. Geosci. Remote Sens.* **2003**, *41*, 1321–1331.
3. Datt, B.; McVicar, T.R.; Van Niel, T.G.; Jupp, D.L.B.; Pearlman, J.S. Preprocessing EO-1 Hyperion hyperspectral data to support the application of agricultural indexes. *IEEE Trans. Geosci. Remote Sens.* **2003**, *41*, 1246–1259.
4. Staenz, K.; Neville, R.A.; Clavette, S.; Landry, R.; White, H.P.; Hitchcock, R. Retrieval of Surface Reflectance from Hyperion Radiance Data. Available online: http://ieeexplore.ieee.org/xpl/login.jsp?tp=&arnumber=1026135&url=http%3A%2F%2Fieeexplore.ieee.org%2Fxppls%2Fabs_all.jsp%3Farnumber%3D1026135 (accessed on 5 September 2014).
5. Pande-Chhetri, R.; Abd-Elrahman, A. De-striping hyperspectral imagery using wavelet transform and adaptive frequency domain filtering. *ISPRS J. Photogramm. Remote Sens.* **2011**, *66*, 620–636.
6. Pande-Chhetri, R.; Abd-Elrahman, A. Filtering high-resolution hyperspectral imagery in a maximum noise fraction transform domain using wavelet-based de-striping. *Int. J. Remote Sens.* **2013**, *34*, 2216–2235.